

## Shell-Model Calculations for $A = 6-14$ Nuclei with a Realistic Interaction\*

Paul S. Hauge<sup>†</sup> and S. Maripuu<sup>†</sup>

*Cyclotron Laboratory, Physics Department, Michigan State University, East Lansing, Michigan 48823*

(Received 20 June 1973)

Shell-model calculations are performed on the normal parity states of  $0p$ -shell nuclei with  $A = 6-14$ . The Hamiltonian is diagonalized in the full  $0p$  basis, and the effective two-body interaction is computed from the Sussex relative harmonic-oscillator matrix elements. The second-order corrections to the two-body matrix elements are calculated for all intermediate states up to  $2\hbar\omega$  excitation energy. The harmonic-oscillator size parameter is taken to be constant at 1.7 fm for all nuclei, and the  $p_{3/2}$ - $p_{1/2}$  single-particle energy splitting is determined for each mass number by a least-squares rms fitting to the experimental spectrum. Static and dynamic properties of the energy levels are calculated and found to be usually in good agreement with experiment.

### I. INTRODUCTION

The basic problem in any feasible shell-model calculation is to determine the effective two-body interaction appropriate for the chosen configuration space. The most appealing method is, of course, to compute this interaction directly from the free nucleon-nucleon scattering phase shifts, without introducing any parameters. The pioneering work of Kuo and Brown,<sup>1-3</sup> using the Hamada-Johnston potential, has yielded very promising results, and today a number of successful shell-model calculations, based on the Kuo-Brown interaction, exist for several nuclear regions.<sup>4,5</sup>

An interesting alternative to the Kuo-Brown method has been suggested by Elliott and his collaborators at Sussex.<sup>6,7</sup> By making some reasonable assumptions about the smoothness and range of the potential, they are able to deduce the relative harmonic-oscillator matrix elements directly from the phase shifts without ever constructing an explicit form for the interaction. In spite of a number of applications with the Sussex matrix elements (see, e.g., Ref. 8), they have rarely been used in any detailed shell-model calculations. In the present work, we shall apply an effective Sussex interaction to the normal parity states of the  $0p$  shell, computing not only energy levels, but also numerous other observables which have been measured and exist in the literature.

Our primary reason for choosing the  $0p$  shell is that a comprehensive investigation of these states, employing realistic two-body forces, has so far not been performed. One previous calculation, using an effective Hamada-Johnston potential, was carried out in this region by Halbert, Kim, and Kuo,<sup>9</sup> but they computed only the energy levels. Some qualitative comparisons with this work will be given in the last section. We shall also compare our results with the successful work

of Cohen and Kurath,<sup>10</sup> who determined their two-body effective interaction by a least-squares fitting of up to 17 free parameters. Even though their method for obtaining an effective interaction is the opposite of ours, it will be shown in the present work that most of our computed observables are very similar to theirs.

Other shell-model calculations have been performed in this region and must be briefly mentioned at this time. For example, the intermediate coupling calculations<sup>11,12</sup> yield quite satisfactory results provided one allows the spin-orbit term to gradually increase throughout the shell. Also, the least-squares technique of Cohen and Kurath has been extended by Goldhammer and co-workers<sup>13</sup> to include some three- and four-body effective forces. In most cases, very good agreement with experiment is obtained.

In Sec. II we present the necessary theory for constructing the Hamiltonian matrices and for computing the effective two-body matrix elements (2BME's). The theoretical energy-level fittings for each nucleus are then presented in Sec. III. We further test the wave functions in Sec. IV by comparing radiative transitions, spectroscopic factors for one-nucleon-transfer reactions, static dipole moments, and  $\beta$ -decay rates with experiment. Finally, in Sec. V we discuss the results and present comparisons with other shell-model calculations.

### II. THEORY

The construction and diagonalization of the energy matrices were performed with the Oak Ridge-Rochester shell-model codes,<sup>14</sup> which require the two-body matrix elements to be expressed in the  $jj$ -coupling scheme. The "bare" two-body matrix elements corresponding to the first diagram of Fig. 1 have been computed from the relative harmonic-oscillator matrix elements tabulated in

Ref. 7. The necessary transformation from  $LS$ - to  $jj$ -coupling, as well as the Brody-Moshinsky transformation between the center-of-mass and relative frame, has been carried out along the lines as described in Ref. 1.

Because of the limited configuration space, we have also computed various corrections to the interaction via degenerate perturbation theory.<sup>15</sup> In the present work, we shall limit our calculations to the second-order terms of all possible  $2\hbar\omega$  corrections. The three possible kinds are shown in Fig. 1 and are commonly referred to as the three-particle-one-hole, four-particle-two-hole, and two-particle corrections, respectively. The explicit formulas for these corrections can be found, for instance, in Ref. 1. There are two types of two-particle corrections that need to be considered, these being (1) both particles excited  $1\hbar\omega$  to the  $1s-0d$  shell, and (2) one particle remaining in the  $0p$  shell and the other excited  $2\hbar\omega$  to the  $0f-1p$  shell.

Numerical values for each of the 15 two-body matrix elements (2BME's) needed in the present calculation are shown in Table I for a representative oscillator length of  $b=1.7$  fm. The "bare" matrix elements are listed in column 2, and the three second-order corrections of Fig. 1 are given in columns 3 through 5. In computing these corrections, we assumed all energy denominators to be exactly  $2\hbar\omega$  (28.4 MeV for  $b=1.7$  fm). By summing columns 2 through 5, we obtain the final effective matrix elements, as tabulated in column 6.

### III. ENERGY LEVELS

In performing the energy-level calculations we at first allowed two parameters to vary, these being (1)  $\epsilon$ , the energy separation between the  $p_{3/2}$

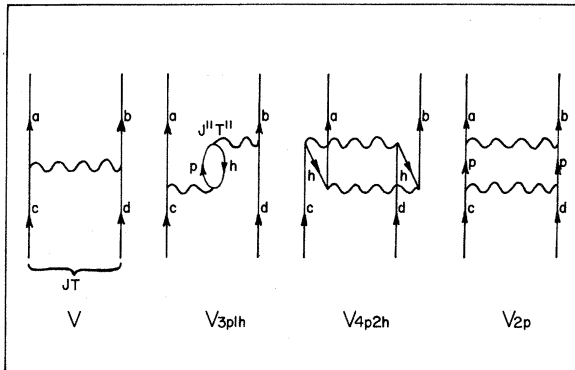


FIG. 1. Diagrams representing the various second-order perturbative corrections to the unperturbed interaction  $V$ .

and  $p_{1/2}$  single-particle states, and (2)  $b$ , the harmonic-oscillator size parameter. The effective 2BME's for the  $0p$  shell were calculated for all oscillator parameters between  $b=1.4$  fm and  $b=1.8$  fm in steps of 0.1 fm. We then computed the normal parity states of the  $0p$  shell for these five values of  $b$  and for different  $\epsilon$  values between 0.0 and 9.0 MeV. Excitation energies were fitted relative to the ground state of each mass number  $A$ . From these results, we observed that the calculated levels varied greatly with  $\epsilon$ , but changed very slowly as a function of  $b$  (with the exception of mass  $A=8$  as will be discussed shortly). Furthermore, it was found that the optimum value of  $b$  was 1.7 fm. Therefore, in the present work, we shall use a constant  $b$  value of 1.7 fm and treat only  $\epsilon$  as a free parameter. This idea of having a constant size parameter for all  $0p$ -shell nuclei is supported by Wilkinson and Mafethe,<sup>16</sup> who have carried out an analysis of three different experimental quantities for all  $0p$ -shell nuclei and found virtually no change in the nuclear size throughout the entire shell.

As seen from Fig. 2, most of our calculated levels are in good agreement with the experimentally observed ones. The optimum values of  $\epsilon$ , which are displayed in Fig. 2 below each theoretical spectrum, were determined to the nearest 0.10 MeV by a  $\chi^2$  fitting procedure. The only experimental states not taken from the standard review articles<sup>17</sup> are the levels at  $E_x=2.9$  MeV in  $^9\text{Be}$ ,  $E_x=8.57$  MeV in  $^{11}\text{B}$ , and  $E_x=10.3$  MeV in

TABLE I. The two-body matrix elements in the form  $\langle ab; JT|V|cd; JT\rangle$  are shown for the  $0p$  shell along with their perturbative corrections. The numbers  $a, b, c$ , and  $d$  represent  $2J_a, 2J_b, 2J_c$ , and  $2J_d$ , respectively. All matrix elements are calculated for the oscillator length parameter  $b=1.7$  fm and expressed in MeV.

$a$	$b$	$c$	$d$	$JT$	$\langle V \rangle$	$\langle V_{3p1h} \rangle$	$\langle V_{4p2h} \rangle$	$\langle V_{2p} \rangle$	$\langle V_{\text{eff}} \rangle$
3	3	3	3	10	-1.541	-0.055	-0.112	-0.838	-2.546
				-30	-4.060	-0.158	...	-0.764	-4.982
				-01	-3.020	-0.276	-0.303	-0.414	-4.013
				-21	-1.453	+0.315	...	-0.170	-1.308
3	3	3	1	10	+3.528	+0.059	+0.316	+0.562	+4.465
				-21	-1.539	-0.276	...	-0.127	-1.942
3	3	1	1	10	+1.676	+0.026	-0.138	+0.437	+2.001
				-01	-3.606	-0.643	-0.214	-0.176	-4.639
3	1	3	1	10	-4.770	+0.196	-0.888	-0.923	-6.385
				-20	-5.350	+0.156	...	-1.255	-6.449
				-11	-0.728	+0.544	...	-0.051	-0.235
				-21	-2.542	+0.522	...	-0.261	-2.281
3	1	1	1	10	+0.942	+0.256	+0.389	-0.174	+1.413
1	1	1	1	10	-1.843	+0.065	-0.170	-0.722	-2.670
				-01	-0.470	+0.264	-0.152	-0.289	-0.647

$^{12}\text{C}$ , which are obtained from more recent papers.<sup>18-20</sup>

It is worth noting that our fitted values of  $\epsilon$  change dramatically in the middle of the shell. For  $A \leq 9$ ,  $\epsilon$  fluctuates between 2.6 and 4.8 MeV, and is reasonably close to the value  $2.6 \pm 0.4$  MeV obtained from the experimental  $^5\text{He}$  spectrum.<sup>17</sup>

For  $A \geq 10$  nuclei, however, the  $\epsilon$  values are considerably higher and are all approximately constant at around 7 MeV.

The most noticeable variance between experiment and theory in Fig. 2 occurs for the lowest  $J^\pi T = 0^+ 1$  states in the  $A = 6, 10,$  and  $14$  nuclei, which are all predicted roughly 2 MeV lower than

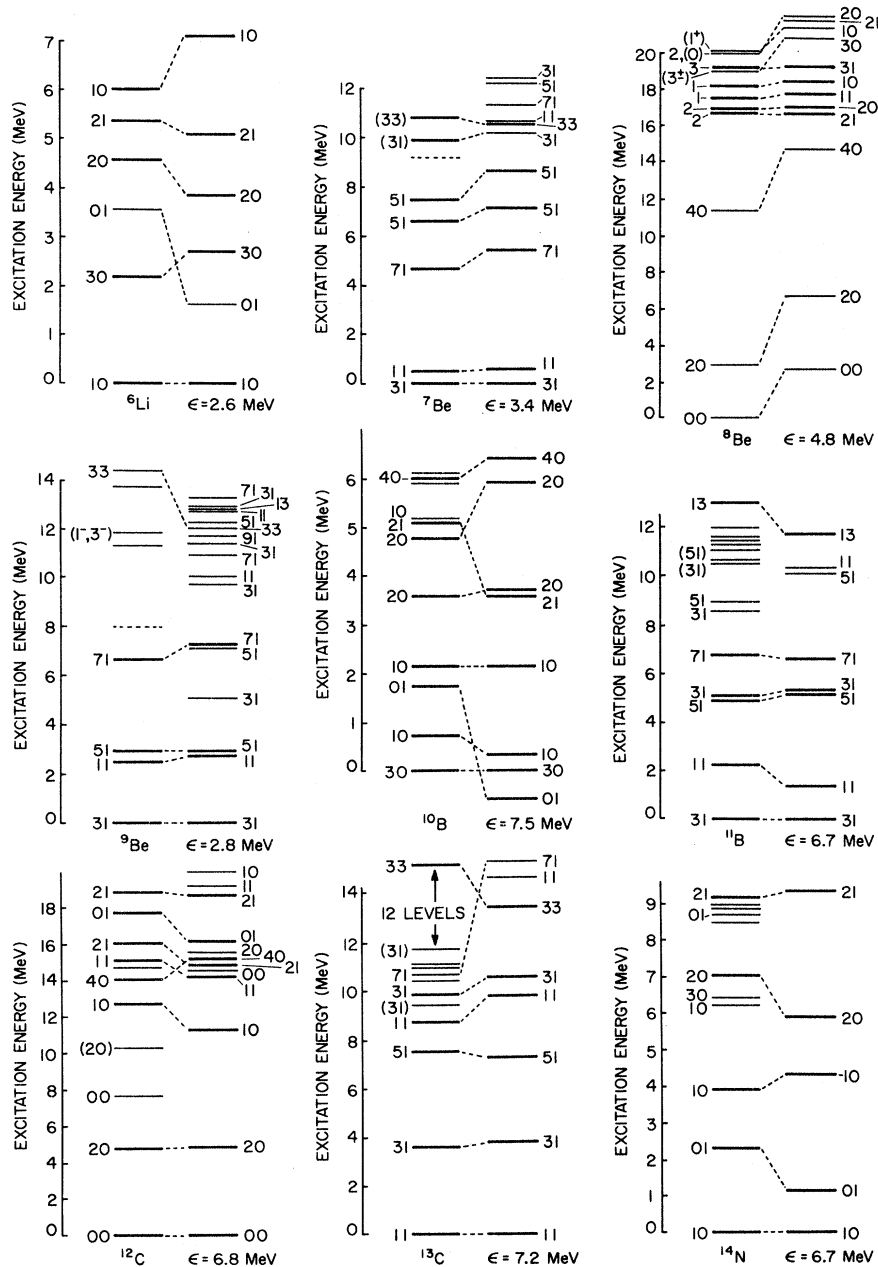


FIG. 2. Comparison of experimental and theoretical shell-model spectra for  $A = 6-14$  nuclei. States are labeled by  $J, T$  for even nuclei and  $2J, 2T$  for odd nuclei. Experimental states with known unnatural parity are not shown. The  $p_{3/2} - p_{1/2}$  separation energy,  $\epsilon$ , is indicated below each calculated spectrum, and the oscillator length is held constant at  $b = 1.7$  fm.

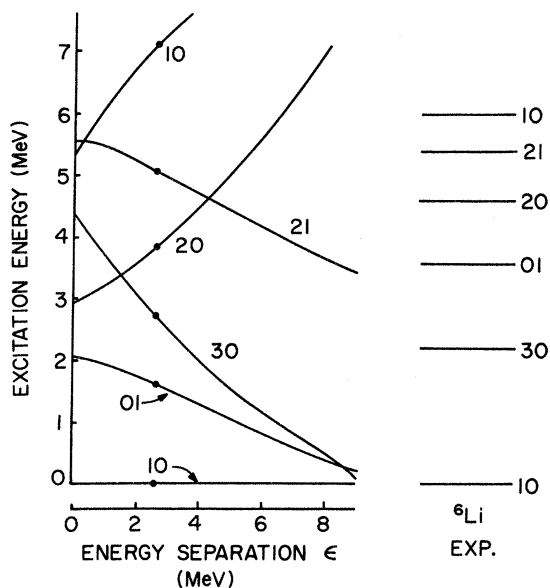


FIG. 3. Diagram showing how the energy levels vary with  $\epsilon$  for  ${}^6\text{Li}$ . The oscillator parameter is held constant at  $b=1.7$  fm. The dots at  $\epsilon=2.6$  MeV indicate the best least-squares fit to experimental data.

their experimental values. We were unable to raise the relative positions of these levels significantly by varying either  $\epsilon$  or  $b$ . This is shown for the  $A=6$  nucleus in Fig. 3, where we see that the  $J^\pi T=0^+1$  state is at least 1.5 MeV below experiment for all positive values of  $\epsilon$ . We cannot give

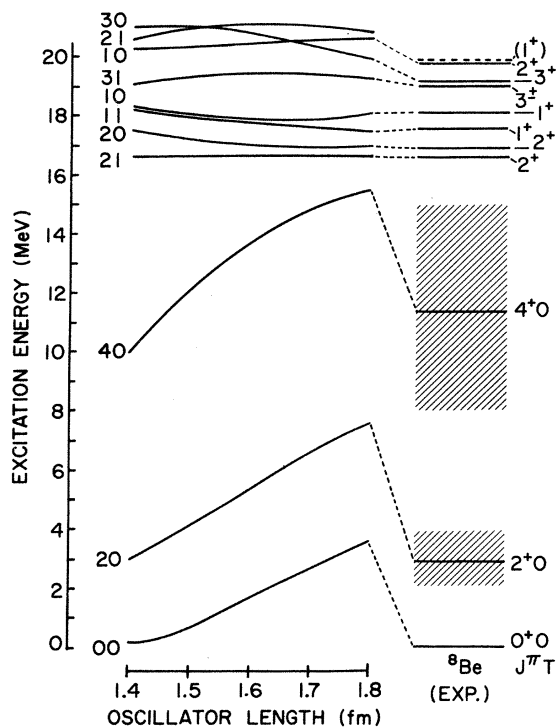


FIG. 4. The theoretical energy levels of  ${}^8\text{Be}$  displayed as a function of the oscillator length  $b$ . The energy separation  $\epsilon$  is held constant at 4.0 MeV. Only those experimental levels of positive or uncertain parity below 20 MeV are shown. The shaded areas of two of the states indicate large reduced widths caused from  $\alpha$  decay. The states above 16 MeV have considerable isospin mixing.

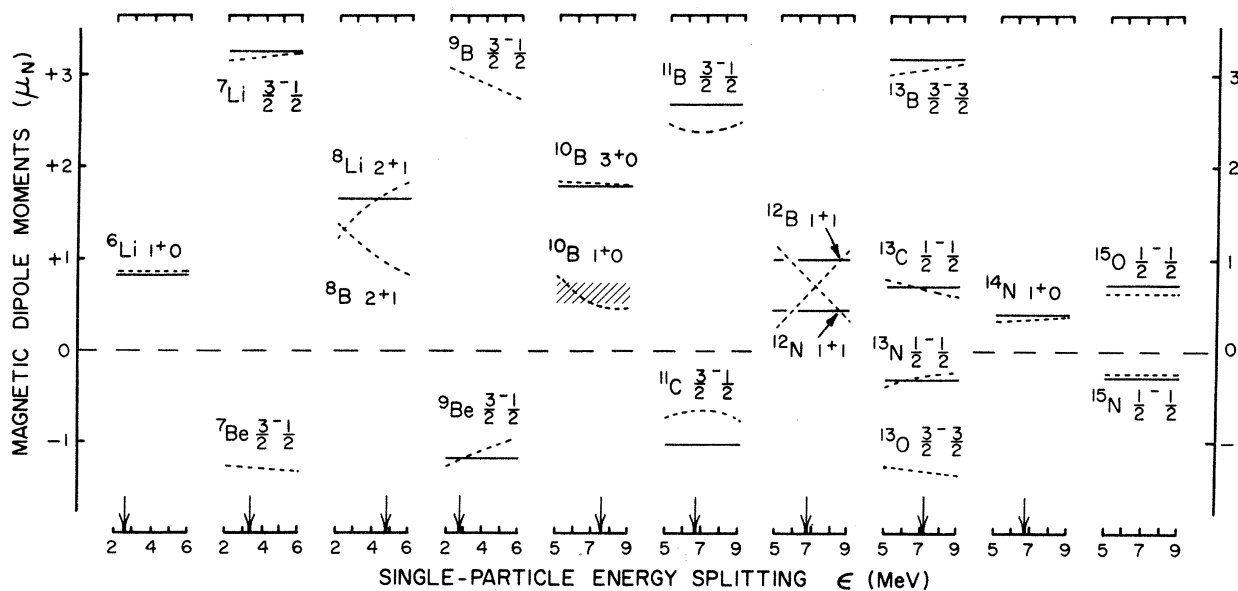


FIG. 5. Magnetic dipole moments for  $0p$ -shell nuclei. Solid lines indicate experimental values, and dashed curves show the theoretical values as a function of  $\epsilon$ . The oscillator length is held constant at  $b=1.7$  fm. The arrows on the horizontal axes indicate the optimum values of  $\epsilon$  determined by the energy-level fittings of the previous section. All moments, except for the  $J^\pi T=1^+0$  state in  ${}^{10}\text{B}$ , are for the ground states of the various nuclei. Notice that the energy scales for nuclei with  $A \geq 10$  are displaced upwards relative to those of  $A \leq 9$  by 3.0 MeV.

a definite explanation for this variance. However, it should be noted that other physical properties connected with these  $J^\pi T = 0^+1$  states are well predicted with the present model, as will be shown in the next section. We have also found that our interaction produces wave functions similar to those of other effective  $0p$ -shell interactions.<sup>10-13</sup>

Another large discrepancy in Fig. 2 occurs for the mass  $A = 8$  spectrum, where we are unable to predict the observed splitting between the lowest

three " $\alpha$ -cluster" states of  ${}^8\text{Be}$  and the other states observed above  $E_x = 16$  MeV. A plausible explanation for this variance is that the lowest three levels, which are known to be highly deformed  $\alpha$ -cluster states, contain relatively large admixtures from shells outside the present configuration space. Consequently, we chose to omit the lowest three states in our fitting procedure, and to normalize our theoretical levels to the experimental  $J^\pi = 2^+$  state at 16.63 MeV. With

TABLE II. Magnetic dipole transitions for normal parity states in odd- $A$  nuclei. The states are characterized by the quantum numbers  $2J, 2T$  and their experimental excitation energies. All states shown have negative parity. Levels followed by the letters A or T signify that the experimental state has not yet been observed, and that the excitation energy is (1) taken from the observed analog state in the mirror nucleus, or (2) computed from the present work, respectively. All theoretical strengths are presented to three significant figures, or five decimal places, whichever comes first.

Nucleus	Final state $2J, 2T [E_x \text{ (MeV)}]$	Initial state $2J, 2T [E_x \text{ (MeV)}]$	$B(M1)$ transition strengths ( $\mu_N^2$ )		
			(6-16)2BME	Present	Experiment
${}^5\text{He}$	31(0.00)	11(2.6)	2.33	2.33	
${}^5\text{Li}$	31(0.00)	11(~4)	3.35	3.35	
${}^7\text{Li}$	31(0.00)	11(0.48)	4.44	4.42	$4.75 \pm 0.24$
		51(6.56)	0.000 64	0.000 36	0.42
		51(7.48)	0.0393	0.0851	$0.184 \pm 0.082$
	11(0.48)	(31)(9.6)	0.0680	0.105	$0.17 \pm 0.09$
		33(11.13)	0.0852	0.0764	
		31(9.6)	0.002 41	0.007 78	
${}^7\text{Be}$	31(0.00)	33(11.13)	0.116	0.225	
		11(0.43)	3.28	3.28	$3.43 \pm 0.33$
		51(6.51)	0.001 08	0.000 03	
	11(0.43)	51(7.19)	0.0461	0.105	
		(31)(9.9)	0.0799	0.139	
		33(10.79)	0.0852	0.0764	
${}^9\text{Be}$	31(0.00)	(31)(9.9)	0.005 83	0.007 97	
		33(10.79)	0.116	0.225	
		51(2.43)	0.404	0.422	$0.745 \pm 0.096$
	51(2.43)	11(2.9)	2.35	2.48	
		31(5.11)T	0.330	0.398	
		51(7.07)T	0.001 77	0.0143	
		33(14.39)	0.201	0.111	
		31(5.11)T	1.84	1.79	
		71(6.66)	0.395	0.334	
		51(7.07)T	0.302	0.376	
11(2.9)	33(14.39)	0.322	0.310	$0.63 \pm 0.13^a$	
	31(5.11)T	0.0541	0.0500		
${}^9\text{B}$	31(0.00)	33(14.39)	0.0251	0.0200	$0.211 \pm 0.051^a$
		51(2.33)	0.495	0.528	
		11(2.9)A	3.30	3.44	
	51(2.33)	31(5.11)T	0.487	0.574	
		51(7.07)T	0.005 44	0.0215	
		33(14.67)	0.201	0.111	
		31(5.11)T	2.59	2.51	
		71(6.66)A	0.455	0.417	
		51(7.07)T	0.425	0.534	
		33(14.67)	0.322	0.310	
11(2.9)A	31(5.11)T	0.0885	0.0903		
	33(14.67)	0.0251	0.0200		

<sup>a</sup> J. C. Adloff, K. H. Souw, and C. L. Cocke, Phys. Rev. C 3, 1808 (1971).

this normalization, we see from Fig. 2 that the three lowest states appear to be about 3 MeV too high. The experimental spectrum of  $^{12}\text{C}$  also contains states (at 7.35 and 10.3 MeV) of presumably  $\alpha$ -cluster nature.<sup>20</sup> We again predict these states several MeV too high, as do other shell-model calculations.<sup>9-13</sup>

As noted earlier, the  $A=8$  system was different from all others considered, in that the computed levels had a strong dependence on the oscillator parameter  $b$ . In Fig. 4 we display the energy levels of  $^8\text{Be}$  as a function of  $b$  ( $\epsilon$  is constant at 4.0 MeV). We notice that the "shell-model" states above  $E_x=16$  MeV remain relatively constant, but that the spacing between these states and the three lower collective states definitely improves as one decreases  $b$  to the value of  $b=1.4$  fm. In lieu of the above discussion, however, we

are forced to conclude that this excellent agreement achieved at  $b=1.4$  fm is quite accidental, and that  $b=1.7$  fm is a more physical value for this nucleus.

For nuclei with mass numbers  $A \geq 11$ , we see from Fig. 2 that there are many low-lying normal parity states between 6 and 12 MeV which are not predicted in our present work. These states are presumed to have large contributions from the  $1s-0d$  shell. Also, it should be noted that for the mass  $A=9$  system we predict two states below 8 MeV which have so far not been observed. We feel confident that these levels do exist, since previous shell-model calculations predict similar states at about the same energy.<sup>10-13</sup> In fact, the first successful observation of the lowest  $J^\pi T = \frac{1}{2}^- \frac{1}{2}$  state in  $^9\text{Be}$  was motivated primarily by early shell-model calculations.<sup>18</sup>

TABLE III. Magnetic dipole transitions for normal parity states in even- $A$  nuclei. The states are characterized by the quantum numbers  $JT$  and their experimental excitation energies. All states shown have positive parity. See caption of Table II for other details.

Nucleus	Final state $JT [E_x \text{ (MeV)}]$	Initial state $JT [E_x \text{ (MeV)}]$	$B(M1)$ transition strengths ( $\mu_N^2$ )		
			(6-16)2BME	Present	Experiment
$^6\text{Li}$	10(0.00)	01(3.56)	15.0	16.4	13.5 $\pm$ 1.0
		20(4.57)	0.00239	0.00045	
		21(5.36)	0.128	0.00760	0.09 $\pm$ 0.08
	30(2.18)	10(6.0)	0.0111	0.00092	
		20(4.57)	0.0323	0.0323	
		21(5.36)	7.56	7.21	
$^8\text{Be}$	01(3.56)	10(6.0)	0.406	0.199	
	00(0.00)	11(17.64)	0.195	0.305	0.26
		10(18.15)	0.00026	0.00087	0.04 $\pm$ 0.04
	20(2.9)	21(16.63)	0.184	0.277	0.063 $\pm$ 0.019
		20(16.93)	0.00055	0.00085	
		11(17.64)	0.0335	0.0885	0.22
		10(18.15)	0.00040	0.00052	0.066
31(19.2)		0.0710	0.163		
$^8\text{Li}$	21(0.00)	30(19.2)	0.00020	0.00052	
		11(0.98)	4.62	5.06	>1.7
		31(2.26)	0.678	0.578	
$^8\text{B}$	21(0.00)	11(0.78)	3.59	3.97	9.1 $\pm$ 4.6
		31(2.17)	0.770	0.707	
$^{10}\text{B}$	30(0.00)	20(3.59)	0.00000	0.0132	0.00132 $\pm$ 0.00024
		20(4.77)	0.0318	0.0201	
		21(5.17)	0.0515	0.00078	0.100 $\pm$ 0.020
		40(6.03)	0.00454	0.00514	0.0069 $\pm$ 0.0012
	10(0.72)	01(1.74)	12.6	6.27	0.39 $\pm$ 0.15
		10(2.15)	0.00511	0.0193	0.0018 $\pm$ 0.0006
		20(3.59)	0.000734	0.0114	0.0119 $\pm$ 0.0022
		20(4.77)	0.00129	0.00566	
		21(5.17)	0.00002	3.41	0.76 $\pm$ 0.16
	01(1.74)	10(2.15)	0.709	2.46	0.105 $\pm$ 0.052
	10(2.15)	20(3.59)	0.0199	0.00534	0.0244 $\pm$ 0.0045
		20(4.77)	0.00138	0.00131	
		21(5.17)	3.37	0.295	6.1 $\pm$ 1.2
		20(3.59)	20(4.77)	0.000395	0.00136
21(5.17)		3.67	1.34	4.17 $\pm$ 0.88	

## IV. TESTING THE WAVE FUNCTIONS

## A. Magnetic Dipole Moments

The magnetic dipole moments were computed by using the "bare" values for the gyromagnetic ratios. The results are shown in Fig. 5 where we display the theoretical moments (dashed curves) as a function of the single-particle energy splitting  $\epsilon$ . All experimental moments are taken from Ref. 17 with the exception of the  $^{12}\text{B}$  ground-state mo-

ment,<sup>21</sup> and the static moment of the  $J^\pi T = 1^+0$  state in  $^{10}\text{B}$  at  $E_x = 0.72$  MeV.<sup>22</sup>

For most mass numbers, there is good agreement between experiment and theory when one uses the values of  $\epsilon$  determined by the energy-level fittings of Sec. III (which are indicated in Fig. 5 by arrows on the horizontal axes). Even the computed dipole moments for the single-hole states of the  $A=15$  nuclei, which might be expected to have large contributions from the  $1s-0d$

TABLE IV. Magnetic dipole transitions for negative-parity states in odd- $A$  nuclei. See caption of Table II for details.

Nucleus	Final state $2J, 2T [E_x \text{ (MeV)}]$	Initial state $2J2T [E_x \text{ (MeV)}]$	$B(M1)$ transition strengths ( $\mu_N^2$ )				
			(6-16)2BME	Present	Experiment		
$^{11}\text{B}$	31(0.00)	11(2.12)	1.80	1.40	$1.198 \pm 0.067$		
		51(4.44)	0.517	0.574	$0.56 \pm 0.25$		
		31(5.02)	1.35	1.39	$1.16 \pm 0.23$		
		31(8.57)	0.002 74	0.123	$0.099 \pm 0.041$		
		51(8.93)	0.384	0.604	$0.525 \pm 0.070$		
	11(2.12)	13(13.02)	0.992	1.47			
		31(5.02)	0.994	0.877	$0.56 \pm 0.11$		
		31(8.57)	0.135	0.352			
	51(4.44)	13(13.02)	0.150	0.0508			
		31(5.02)	2.79	2.22			
		71(6.74)	0.0118	0.0390			
		31(8.57)	0.108	0.604			
51(8.93)		0.008 48	0.0307	0.0072			
$^{11}\text{C}$	31(0.00)	11(2.00)	1.22	0.888			
		51(4.31)	0.359	0.390			
		31(4.79)	0.994	1.00			
		31(8.11)	0.000 17	0.188			
		51(8.42)	0.493	0.778			
	11(2.00)	13(12.45)	0.992	1.47			
		31(4.79)	0.808	0.691			
		31(8.11)	0.0848	0.312			
	51(4.31)	13(12.45)	0.150	0.0508			
		31(4.79)	2.06	1.59			
		71(6.48)	0.0182	0.0552			
		31(8.11)	0.154	0.769			
51(8.42)		0.0214	0.0570				
$^{13}\text{C}$	11(0.00)	31(3.68)	1.19	0.906	$0.763 \pm 0.070$		
		11(8.86)	0.913	1.06			
		31(9.90)	0.272	0.565			
		33(15.11)	0.734	0.884			
		51(7.55)	0.004 65	0.001 72			
	31(3.68)	11(8.86)	0.000 06	0.009 57			
		31(9.90)	0.220	0.0112			
		33(15.11)	0.522	1.22			
		$^{13}\text{N}$	11(0.00)	31(3.51)	1.62	1.34	1.32
				11(8.92)	0.714	0.800	
31(9.52)	0.130			0.347			
31(3.51)	33(15.07)		0.734	0.884			
	51(7.39)		0.003 83	0.001 27			
	11(8.92)		0.0163	0.000 05			
	31(9.52)	0.220	0.008 81				
	33(15.07)	0.522	1.22				

shell, are very close to their experimental values. The worst discrepancy occurs for the mass  $A=11$  nuclei.

### B. $M1$ Transitions

Because of the over-all excellent agreement between the experimental and theoretical dipole moments, we again use the "bare"  $g$  factors in computing the  $M1$  transition probabilities. Our present calculations are compared not only with experiment, but also with the strengths determined from the (6-16)2BME interaction of Cohen and Kurath<sup>10</sup> (hereafter referred to as CK). The results for the lower half of the  $0p$  shell are displayed in Tables II and III for odd  $A$  and even  $A$ , respectively. Even though our method of computing the effective interaction is completely different from CK's approach, we see from the correspondence between the two theoretical transition strengths that our wave functions are very similar. The primary exception to this over-all agreement occurs for the  $^{10}\text{B}$  nucleus in Table III, where we find large deviations between the two theories, as well as between both theories and experiment, for the transitions involving the lowest  $J^\pi T = 1^+0$

states at 0.72 and 2.15 MeV. In our present work, we find that these two eigenvectors almost completely exchange their wave-function components between  $\epsilon=5$  and  $\epsilon=8$  MeV, and thus we conclude that the character of these two eigenvectors is largely undetermined in both theoretical calculations. Indeed, Warburton *et al.*<sup>23</sup> have studied this problem in detail by comparing CK's (8-16) POT wave functions with  $M1$  and  $E2$  transition probabilities, as well as several  $E2/M1$  mixing ratios. They find that a 16% mixing in intensities for both the lowest two  $J^\pi T = 1^+0$  and  $2^+0$  wave functions in  $^{10}\text{B}$  yields theoretical numbers that are in much better agreement with experiment. The transition strengths for nuclei in the upper half of the  $0p$  shell are displayed in Tables IV and V for odd  $A$  and even  $A$ , respectively. Again, we find good agreement for most of the levels considered, even though we might expect  $(sd)^2$  components in some of the wave functions.

All transition strengths in Tables II through V are given in  $\mu_N^2$ , and must be multiplied by the factor 0.56 ( $\approx 8\pi/45$ ) in order to be expressed in terms of Weisskopf units.<sup>24</sup> The experimental values presented for some of the transitions are

TABLE V. Magnetic dipole transitions for positive-parity states in even- $A$  nuclei. See caption of Table III for details.

Nucleus	Final state $JT [E_x \text{ (MeV)}]$	Initial state $JT [E_x \text{ (MeV)}]$	$B(M1)$ transition strengths ( $\mu_N^2$ )		
			(6-16)2BME	Present	Experiment
$^{12}\text{C}$	00(0.00)	10(12.21)	0.004 60	0.004 57	
		11(15.11)	0.816	0.969	1.100 $\pm$ 0.079
	20(4.44)	10(12.71)	0.002 43	0.002 90	
		11(15.11)	0.0301	0.0660	0.33 $\pm$ 0.14
		21(16.11)	0.543	0.542	0.369 $\pm$ 0.060
		21(18.84)	0.166	0.328	
	10(12.71)	20(15.58)T	0.002 09	0.002 73	
		11(15.11)	2.80	2.59	
		21(16.11)	0.265	0.134	
		01(17.77)	6.65	5.60	
21(18.84)		1.96	1.97		
$^{12}\text{B}$	11(0.00)	21(0.95)	0.269	0.194	0.195 $\pm$ 0.057
		01(2.72)	0.162	0.176	
		21(3.76)	0.166	0.276	
	21(0.95)	21(3.76)	0.555	0.143	
$^{12}\text{N}$	11(0.00)	21(0.97)	0.154	0.119	
		01(2.72)A	0.710	0.711	
		21(3.76)A	0.0495	0.0987	
	21(0.00)	21(3.76)A	0.747	0.241	
$^{14}\text{N}$	10(0.00)	01(2.31)	0.003 12	0.0693	0.0582 $\pm$ 0.0086
		10(3.95)	0.000 05	0.001 76	0.000 82 $\pm$ 0.000 17
		20(7.03)	0.0277	0.0275	0.0221 $\pm$ 0.0040
		21(9.17)	2.96	2.91	0.975
	01(2.31)	10(3.95)	3.42	2.97	2.78 $\pm$ 0.26
	10(3.95)	20(7.03)	0.000 24	0.001 00	
		21(9.17)	0.0195	0.0669	

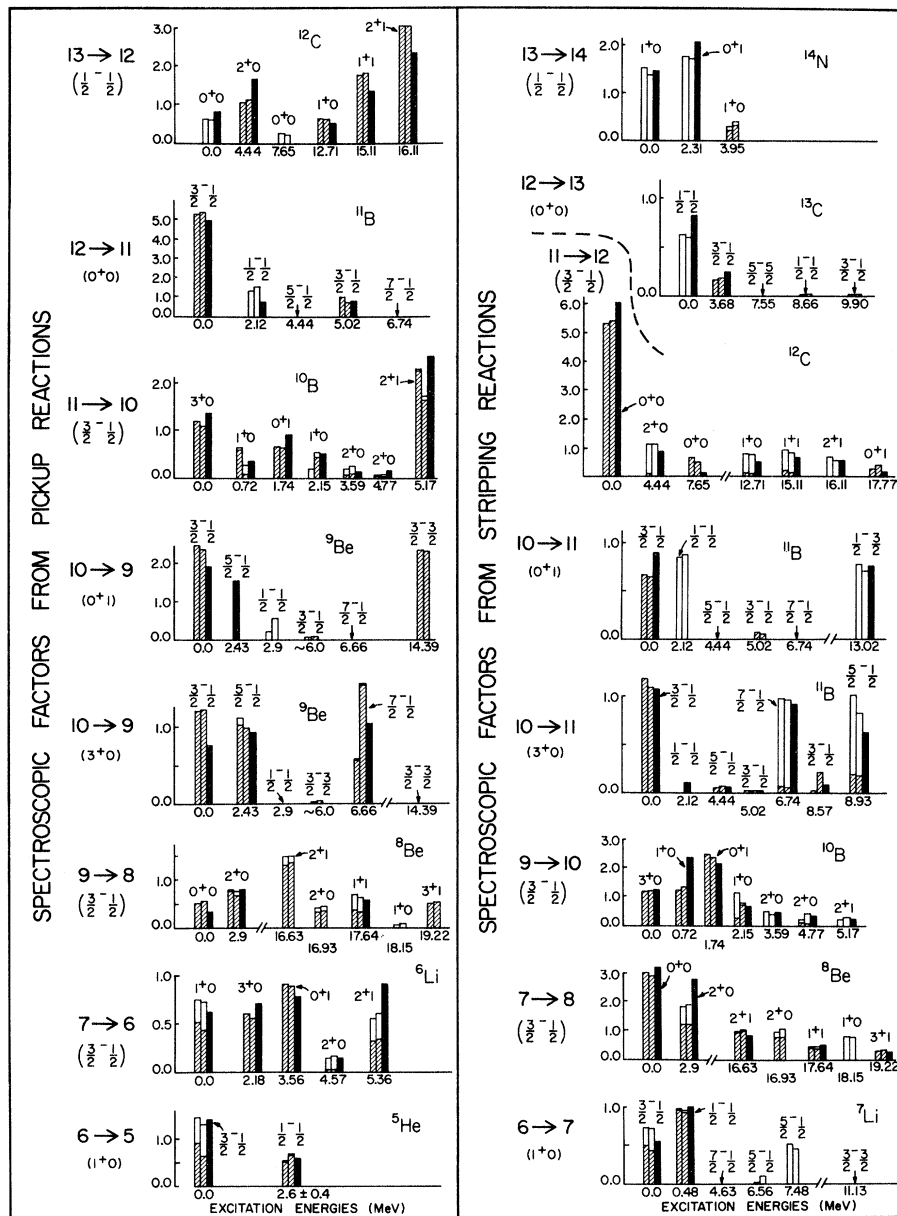


FIG. 6. Single-nucleon spectroscopic factors of the  $0p$ -shell nuclei for both pickup and stripping reactions. The mass numbers of the target and residual nuclei, as well as the spin-isospin for the ground state of the target nucleus, are presented to the left of each graph. Each of the possible final states is then displayed along an energy axis, and is designated by both its spin-isospin quantum number and its experimental excitation energy in the residual nucleus. The first two bars for each transition indicate the magnitude of the spectroscopic factors predicted by the present work and by CK (Ref. 25), respectively. The shaded and nonshaded areas of the bars indicate contributions from transferring a nucleon from the  $p_{3/2}$  and  $p_{1/2}$  single-particle orbitals, respectively. Experimental spectroscopic factors, which are presented for some of the transitions as solid bars, were determined from the following papers: For pickup reactions: Refs. 26, 27 for  $A=6$  and  $A=7$  targets; Refs. 12, 26–28 for the  $A=9$  target; Refs. 26, 28–31 for the two  $A=10$  targets; Refs. 26, 28, 31, 32 for the  $A=11$  target; Refs. 26, 33, 34 for the  $A=12$  target; and Ref. 35 for the  $A=13$  target. For stripping reactions: Ref. 36 for the  $A=6$  target; Refs. 12, 36 for the  $A=7$  target; Refs. 36, 37 for the  $A=9$  target; Refs. 29, 33, 36, 38 for the two  $A=10$  targets; Refs. 36, 37, 39 for the  $A=11$  target; and Refs. 36, 40 for the  $A=12$  target.

TABLE VI. Comparison of theoretical and experimental  $\log ft$  values for allowed Gamow-Teller  $\beta$  decays. An asterisk indicates that the state involved has same  $JT$  quantum numbers as that of a lower level.

$A_0(J_0T_0) \rightarrow A(JT)$	(6-16)2BME	Present work	Experiment
${}^6\text{He}(01) \rightarrow {}^6\text{Li}(10)$	2.88	2.86	2.904
${}^7\text{Be}(\frac{3}{2}^+) \rightarrow {}^7\text{Li}(\frac{1}{2}^+)$	3.49	3.50	3.538
${}^8\text{He}(02) \rightarrow {}^8\text{Li}(11)$	4.26	4.01	$4.0 \pm 0.4$
${}^6\text{Li}(21) \rightarrow {}^6\text{Be}(20)$	5.27	5.00	$\left\{ \begin{array}{l} 5.617 \\ 5.657 \end{array} \right.$
${}^8\text{B}(21) \rightarrow {}^8\text{Be}(20)$			
${}^9\text{Li}(\frac{3}{2}^+) \rightarrow {}^9\text{Be}(\frac{3}{2}^+)$	5.05	5.54	$5.12 \pm 0.02^a$ $5.5 \pm 0.2^b$
$\rightarrow {}^9\text{Be}(\frac{3}{2}^+)$	5.10	5.07	$5.00 \pm 0.05^a$ $5.2 \pm 0.2^b$
$\rightarrow {}^9\text{Be}(\frac{1}{2}^+)$	5.40	5.42	$5.97 \pm 0.2^a$ $5.2 \pm 0.2^b$
$\rightarrow {}^9\text{Be}(\frac{3}{2}^+)^*$	6.65	5.81	
$\rightarrow {}^9\text{Be}(\frac{3}{2}^+)^*$	4.44	4.58	
${}^{10}\text{C}(01) \rightarrow {}^{10}\text{B}(10)$	2.93	3.46	$3.055 \pm 0.002$
$\rightarrow {}^{10}\text{B}(10)^*$	4.11	3.10	$\geq 3.9^c$
${}^{12}\text{B}(11) \rightarrow {}^{12}\text{C}(00)$	4.12	4.04	$\left\{ \begin{array}{l} 4.075 \pm 0.02 \\ 4.117 \pm 0.02 \end{array} \right.$
${}^{12}\text{N}(11) \rightarrow {}^{12}\text{C}(00)$			
${}^{12}\text{B}(11) \rightarrow {}^{12}\text{C}(20)$	5.07	4.84	$\left\{ \begin{array}{l} 5.10 \pm 0.03 \\ 5.06 \pm 0.04 \end{array} \right.$
${}^{12}\text{N}(11) \rightarrow {}^{12}\text{C}(20)$			
${}^{12}\text{B}(11) \rightarrow {}^{12}\text{C}(00)^*$	3.53	3.58	$\left\{ \begin{array}{l} 4.14 \pm 0.10 \\ 4.34 \pm 0.06 \end{array} \right.$
${}^{12}\text{N}(11) \rightarrow {}^{12}\text{C}(00)^*$			
${}^{12}\text{N}(11) \rightarrow {}^{12}\text{C}(10)$	3.65	3.70	$3.54 \pm 0.15$
${}^{13}\text{B}(\frac{3}{2}^+) \rightarrow {}^{13}\text{C}(\frac{1}{2}^+)$	3.90	3.82	$4.02 \pm 0.02$
$\rightarrow {}^{13}\text{C}(\frac{3}{2}^+)$	4.80	4.12	$4.47 \pm 0.05$
$\rightarrow {}^{13}\text{C}(\frac{5}{2}^+)$	5.24	4.63	$5.37 \pm 0.09$
$\rightarrow {}^{13}\text{C}(\frac{1}{2}^+)^*$	4.40	4.87	$4.63 \pm 0.08$
$\rightarrow {}^{13}\text{C}(\frac{3}{2}^+)^*$	4.02	3.77	
${}^{14}\text{C}(01) \rightarrow {}^{14}\text{N}(10)$	4.92	4.32	$\left\{ \begin{array}{l} 9.03 \\ 7.330 \pm 0.006 \end{array} \right.$
${}^{14}\text{O}(01) \rightarrow {}^{14}\text{N}(10)$			
${}^{14}\text{O}(01) \rightarrow {}^{14}\text{N}(10)^*$	2.94	3.00	$3.08 \pm 0.06$

<sup>a</sup> Y. S. Chen, T. A. Tombrello, and R. W. Kavanagh, Nucl. Phys. **A146**, 136 (1970).

<sup>b</sup> Reference 18.

<sup>c</sup> J. M. Freeman, J. G. Jenken, and G. Murray, Phys. Lett. **22**, 177 (1966).

taken from (1) energy level reviews,<sup>17</sup> (2) a compilation of electromagnetic transitions for  $A \leq 40$  nuclei,<sup>24</sup> and/or (3) recent experiments not included in the review articles. For the latter case, references are listed at the bottom of the tables.

### C. Gamow-Teller Matrix Elements

In Table VI, we compare experimental and theoretical values of  $\log ft$  for allowed Gamow-Teller  $\beta$  decays. All experimental numbers are taken from the nuclear data review articles of Ref. 17, except for those otherwise referenced in the table. We again present not only our results, but those of CK's (6-16)2BME case,<sup>10</sup> for means of comparison. We see that both sets of theoretical numbers are in good agreement with each other, as well as experiment. The largest discrepancy occurs for the theoretical  $\log ft$  transitions from  ${}^{14}\text{C}$  and  ${}^{14}\text{O}$  to the ground state of  ${}^{14}\text{N}$ , which are much smaller than experiment. However, as has been pointed out by CK,<sup>10</sup> these weak  $\beta$  decays are very sensitive to the details of the wave functions, and

they therefore do not present any serious disagreement between experiment and theory.

### D. Single-Nucleon Spectroscopic Factors

The first systematic tabulation of theoretical spectroscopic factors for  $0p$ -shell nuclei was performed in 1967 by CK<sup>25</sup> using their wave functions of Ref. 10. However, no attempt was made by them to compare their results with the meager data available at that time. In recent years, however, a wealth of experimental information has been obtained, and we shall therefore compare our present calculations to experiment, as well as to CK's theoretical numbers of Ref. 25. The results are displayed, by means of bar diagrams, in Fig. 6. The experimental spectroscopic factors were found by analyzing the results of numerous papers on both pickup<sup>26-35</sup> and stripping<sup>36-40</sup> reactions. One should be careful in not placing too much emphasis on the apparent over-all good agreement between experiment and theory, since some of the experimental papers derived only relative spectroscopic factors and hence normalized their ground-state transitions to those of CK's theoretical values.<sup>25</sup> It is very encouraging, however, to see the excellent agreement between our theoretical values and those of CK's. As was the case for the  $M1$  transitions, the largest variance between the two theories occurs for transitions involving the lowest two  $J^\pi T = 1^+0$  states of  ${}^{10}\text{B}$ . Also, the very small theoretical spectroscopic factors to the second  $J^\pi T = \frac{3}{2}^- \frac{1}{2}$  state in the mass  $A=9$  system help explain why the level has not yet been observed. This level is theoretically predicted by numerous shell-model calculations<sup>10,12,13</sup> to be around  $E_x = 6$  MeV. The largest discrepancy between experiment and theory in Fig. 6 occurs for the pickup reaction from the  $J^\pi T = 0^+1$  ground state in  ${}^{10}\text{Be}$  to the  $J^\pi T = \frac{5}{2}^- \frac{1}{2}$  state in  ${}^9\text{Be}$ . Since the theoretical spectroscopic factor for this transition is zero from angular momentum coupling alone, the large observed cross section (cf., Fig. 6) must proceed by indirect processes.

### V. CONCLUSIONS

Our present calculations have shown that a realistic interaction can satisfactorily explain the properties of most normal parity states in the  $0p$  shell, provided we allow the single-particle energy splitting  $\epsilon$  to vary for each mass number  $A$ . All three types of second-order corrections (cf., Fig. 1 and Table I) are found to be important in determining the effective interaction. The fact that we empirically find the harmonic-oscillator size parameter  $b$  to be relatively constant at 1.7 fm is significant, and helps explain why the

many-parameter fitting procedures of Refs. 10 and 13 are so highly successful.

A comparison of our energy-level fitting procedure with that of Halbert, Kim, and Kuo's<sup>9</sup>  $0p$ -shell calculation using the realistic Hamada-Johnston potential is also quite informative. For example, these authors also find (as we do in the present work) that the seemingly unphysical value of  $b = 1.4$  fm yields the best results for the mass  $A = 8$  spectrum. Such similarities as these indicate that the Sussex and Hamada-Johnston poten-

tials are very similar in nature, even though the Sussex 2BME's are much easier to compute.<sup>1,7</sup>

For heavier mass regions, it is virtually impossible to use the many-parameter least-squares method of CK. Consequently, for most heavy nuclei one must either employ a realistic interaction or use a few-parameter Hamiltonian, such as the modified surface  $\delta$  interaction.<sup>41</sup> Investigations are presently underway involving the effective Sussex interaction in several of these mass regions.<sup>42</sup>

\*Work supported in part by the National Science Foundation.

†Part of this work was performed while the authors were National Academy of Sciences-National Research Council Research Associates at the Aerospace Research Laboratories of Wright Patterson Air Force Base, Ohio 45433.

<sup>1</sup>T. T. S. Kuo and G. E. Brown, Nucl. Phys. 85, 40 (1966).

<sup>2</sup>T. T. S. Kuo, Nucl. Phys. A103, 71 (1967).

<sup>3</sup>G. E. Brown and T. T. S. Kuo, Nucl. Phys. A92, 481 (1967); T. T. S. Kuo and G. E. Brown, *ibid.* A114, 241 (1968).

<sup>4</sup>E. C. Halbert, in *Proceedings of the Third Symposium on the Structure of Low-Medium Mass Nuclei, University of Kansas, 1968*, edited by J. P. Davidson (Univ. of Kansas Press, Lawrence, Kansas, 1968), pp. 128-166.

<sup>5</sup>E. C. Halbert, J. B. McGrory, B. H. Wildenthal, and S. P. Pandya, in *Advances in Nuclear Physics*, edited by M. Baranger and E. Vogt (Plenum, New York, 1969), Vol. 4, pp. 315-442.

<sup>6</sup>J. P. Elliot, in *Proceedings of the Third Symposium on the Structure of Low-Medium Mass Nuclei, University of Kansas, 1968* (see Ref. 4), pp. 48-72.

<sup>7</sup>J. P. Elliot, A. D. Jackson, H. A. Mavromatis, E. A. Sanderson, and B. Singh, Nucl. Phys. A121, 241 (1968).

<sup>8</sup>B. S. Cooper, J. B. Seaborn, and S. A. Williams, Phys. Rev. C 4, 1997 (1971).

<sup>9</sup>E. C. Halbert, Y. E. Kim, and T. T. S. Kuo, Phys. Lett. 20, 657 (1966).

<sup>10</sup>S. Cohen and D. Kurath, Nucl. Phys. 73, 1 (1965).

<sup>11</sup>D. R. Inglis, Rev. Mod. Phys. 25, 390 (1953); D. Kurath, Phys. Rev. 101, 216 (1956); *ibid.* 106, 975 (1957).

<sup>12</sup>F. C. Barker, Nucl. Phys. 83, 418 (1966).

<sup>13</sup>J. L. Norton and P. Goldhammer, Nucl. Phys. A165, 33 (1971); P. Goldhammer, J. R. Hill, and J. Nachamkin, *ibid.* A106, 62 (1968); S. Varma and P. Goldhammer, *ibid.* A125, 193 (1969).

<sup>14</sup>J. B. French, E. C. Halbert, J. B. McGrory, and S. S. M. Wong, in *Advances in Nuclear Physics* (see Ref. 5), Vol. 3, pp. 193-257.

<sup>15</sup>B. H. Brandow, Rev. Mod. Phys. 39, 771 (1967).

<sup>16</sup>D. H. Wilkinson and M. E. Mafethe, Nucl. Phys. 85, 97 (1966).

<sup>17</sup>T. Lauritsen and F. Ajzenberg-Selove, Nucl. Phys. 78, 1 (1966); F. Ajzenberg-Selove and T. Lauritsen, Nucl. Phys. A114, 1 (1968); F. Ajzenberg-Selove, *ibid.* A152, 1 (1970).

<sup>18</sup>B. E. F. Macefield, B. Wakefield, and D. H. Wilkinson, Nucl. Phys. A131, 250 (1969).

<sup>19</sup>H. T. Fortune, J. R. Comfort, J. V. Maher, and B. Zeidman, Phys. Rev. C 2, 425 (1970).

<sup>20</sup>H. Morinaga, Phys. Lett. 21, 78 (1966).

<sup>21</sup>K. Sugimoto, K. Nakai, K. Matuda, and T. Minamisono, J. Phys. Soc. Jap. 25, 1258 (1968).

<sup>22</sup>R. Avida, I. Ben-zvi, G. Goldring, S. S. Hanna, P. N. Tandon, and Y. Wolfson, Nucl. Phys. A182, 359 (1972).

<sup>23</sup>E. K. Warburton, J. W. Olness, S. D. Bloom, and A. R. Poletti, Phys. Rev. 171, 1178 (1968).

<sup>24</sup>S. J. Skorka, J. Hertel, and T. W. Retz-Schmidt, Nucl. Data A2, 347 (1966).

<sup>25</sup>S. Cohen and D. Kurath, Nucl. Phys. A101, 1 (1967).

<sup>26</sup>D. Bachelier, M. Bernas, I. Brissaud, C. Detraz, and P. Radvanyi, Nucl. Phys. A126, 60 (1969).

<sup>27</sup>L. A. Kull, Phys. Rev. 163, 1066 (1967).

<sup>28</sup>W. Fitz, R. Jahr, and R. Santo, Nucl. Phys. A101, 449 (1967).

<sup>29</sup>D. L. Auton, Nucl. Phys. A157, 305 (1970).

<sup>30</sup>G. T. A. Squier, A. R. Johnston, E. W. Spiers, S. A. Harbison, and N. M. Stewart, Nucl. Phys. A141, 158 (1970).

<sup>31</sup>L. A. Kull and E. Kashy, Phys. Rev. 167, 963 (1968).

<sup>32</sup>D. Dehnhard, N. Williams, and J. L. Yntema, Phys. Rev. 180, 967 (1969).

<sup>33</sup>W. Bohne, J. Bommer, H. Fuchs, K. Grabisch, M. Hagen, H. Homeyer, U. Janetzki, H. Lettau, H. Morgenstern, G. Roschert, and J. Scheer, Nucl. Phys. A157, 593 (1970).

<sup>34</sup>T. J. Gray, H. T. Fortune, W. Trost, and N. R. Fletcher, Nucl. Phys. A144, 129 (1970).

<sup>35</sup>H. Taketani, J. Mato, H. Yamaguchi, and J. Kokame, Phys. Lett. 27B, 625 (1968).

<sup>36</sup>J. P. Schiffer, G. C. Morrison, R. H. Siemssen, and B. Zeidman, Phys. Rev. 164, 1274 (1967).

<sup>37</sup>M. A. Crosby and J. C. Legg, Nucl. Phys. A95, 639 (1967).

<sup>38</sup>J. R. Comfort, H. T. Fortune, J. V. Maher, and B. Zeidman, Phys. Rev. C 3, 1086 (1971).

<sup>39</sup>G. M. Reynolds, D. E. Rundquist, and R. M. Pochar, Phys. Rev. C 3, 442 (1971); J. E. Monahan, H. T. Fortune, C. M. Vincent, *ibid.* 3, 2192 (1971); P. D. Miller, J. L. Duggan, M. M. Duncan, R. L. Dangle, W. R. Coker, and J. Lin, Nucl. Phys. A136, 229 (1969).

<sup>40</sup>H. Guratzsch, G. Hofmann, H. Muller, and G. Stiller, Nucl. Phys. A129, 405 (1969); H. T. Fortune, T. J.

- Gray, W. Trost, and N. R. Fletcher, *Phys. Rev.* 179, 1033 (1969); C. A. Pearson, J. M. Covan, D. Zissermann, T. G. Miller, F. P. Gibson, R. Haglund, W. Morrison, and G. Westley, *Nucl. Phys.* A191, 1 (1972).
- <sup>41</sup>R. Arvieu and S. A. Moszkowski, *Phys. Rev.* 145, 830 (1966); P. W. M. Glaudemans, P. J. Brussard, and B. H. Wildenthal, *Nucl. Phys.* A102, 593 (1967).
- <sup>42</sup>S. Maripuu, in *Fifth Symposium on Nuclear Structure of Low-Medium Mass Nuclei*, University of Kentucky, 26-28 October, 1972 (University of Kentucky Press, Lexington, Kentucky, to be published); S. Maripuu, B. H. Wildenthal, and A. O. Ewwaraye, *Phys. Lett.* 43B, 368 (1973).